Desalination and Water Treatment
www.deswater.com
doi: 10.1080/19443994.2015.1035676

57 (2016) 9799–9812
May

Taylor & Francis
Taylor & Francis Group

Removal of copper, nickel, lead, and zinc using chitosan-coated montmorillonite beads in single- and multi-metal system

Wan-Chi Tsai[a], Sonia Ibarra-Buscano[b], Chi-Chuan Kan[c], Cybelle Morales Futalan[d], Maria Lourdes P. Dalida[e], Meng-Wei Wan[f,*]

[a]*Department of Medical Laboratory Science and Biotechnology, Kaohsiung Medical University, Kaohsiung 80708, Taiwan, email: carcinogen.tw@yahoo.com.tw*
[b]*Department of Chemical Engineering, University of Philippines-Diliman, Quezon City 1800, Philippines, email: sbib_onxy@yahoo.com*
[c]*Institute of Hot Spring Industry, Chia Nan University of Pharmacy and Science, Tainan 71710, Taiwan, email: cckanev@mail.chna.edu.tw*
[d]*Operations Department, Frontier Oil Corporation, Makati City 1229, Philippines, email: cmfutalan@gmail.com*
[e]*Department of Chemical Engineering, University of Philippines-Diliman, Quezon City 1800, Philippines, email: mpdalida@gmail.com*
[f]*Department of Environmental Engineering and Science, Chia Nan University of Pharmacy and Science, Tainan 71710, Taiwan, Tel. +886 6 266 0615; Fax: +886 6 213 1291; email: peterwan@mail.cnu.edu.tw*

Received 17 August 2014; Accepted 17 March 2015

ABSTRACT

In this study, the removal of Cu(II), Ni(II), Pb(II), and Zn(II) from aqueous solution in single and multi-metal system using chitosan-coated montmorillonite (ChiMC) beads was investigated. The non-crosslinked and crosslinked ChiMC beads were characterized using SEM–EDX, Fourier transform infrared, and Brunauer, Emmett, and Teller analysis. The effect of ionic strength and pH on the adsorption capacity and percent (%) removal of ChiMC was examined. Kinetic studies revealed that adsorption using ChiMC follows the pseudo-second-order equation with high correlation coefficient values ($R^2 > 0.95$). The equilibrium data were correlated with Langmuir and Freundlich isotherm models, where crosslinked ChiMC provided higher maximum adsorption capacity over ChiMC. The calculated Langmuir adsorption capacities for Cu(II), Ni(II), Pb(II), and Zn(II) using ChiMC in single-metal system are 13.04, 12.18, 29.85, and 13.50 mg/g, respectively. An increase in the calculated adsorption capacities derived from Langmuir isotherm was observed in multi-metal system, indicating a synergistic effect. The adsorption capacity in single- and multi-metal system followed the order: Pb(II) > Cu(II) > Zn(II) > Ni(II). The kinetic rate and adsorption capacity of the four metals were observed to increase in multi-metal systems. The removal of Cu(II), Ni(II), Pb(II), and Zn(II) from groundwater by adsorption onto ChiMC was also investigated.

Keywords: Chitosan; Groundwater; Hydrated ionic radius; Ionic strength; Multi-metal system

*Corresponding author.

1. Introduction

Heavy metal contamination in surface and groundwater has been a major concern due to its non-biodegradability and acute toxicity effects on public health and the environment. The presence of heavy metals in waste effluents is generated by several anthropogenic sources such as agricultural use of pesticide and fungicide, paper and pulp industry, mining activities, smelting processes, battery manufacturing, and oil refining [1–3]. Conventional methods used in removing heavy metal from industrial effluents are chemical precipitation, ion exchange, electrodeposition, evaporation, and membrane separation [4]. These technologies have certain drawbacks such as being costly and ineffective in removing heavy metals at dilute concentration [5,6]. In addition, chemical methods generate sludge, which requires proper confinement and disposal [7].

Among the physicochemical treatments, adsorption using activated carbon in the removal of heavy metals and dyes has been employed [8]. Materials of biological origin have been considered as an alternative to the conventional treatment of wastewater containing heavy metals. Natural adsorbents, such as clay materials [9], coconut shell [7], chitin, and chitosan [10,11] are industrially attractive due to their low cost, availability, and capacity of lowering the heavy metal concentration to parts per billion.

Chitosan, a natural amino polysaccharide that contains reactive amine and hydroxyl groups, is obtained from deacetylation of chitin [12,13]. It is widely regarded due to its high adsorption capacity with valuable properties such as nontoxicity, hydrophilicity, biocompatibility, and antibacterial properties [14]. However, chitosan application is limited due to its low surface area, solubility in most mineral and organic acids, and has the tendency to form gel in aqueous media [15]. Therefore, raw chitosan is either physically or chemically modified in the attempt to cause expansion of the polymer network onto an immobilized support, to reduce its crystallinity, and to enhance its mechanical resistance and chemical stability in acidic media [16–18].

Previous studies were made on chitosan support material, which includes sand [14], bentonite [19–21], PVC [6], and perlite [22]. Montmorillonite, a smectite clay mineral composed of three layers, has a 2:1 ratio of Si^{4+} tetrahedral to Al^{3+} octahedral sheets. It is an attractive support material and well-known adsorbent due to its high surface area, mechanical and chemical stability, high cation-exchange capacity, and low cost [23]. In this investigation, physical modification through the process of coating chitosan on the surface of montmorillonite would help overcome the mass transfer limitations and increase the accessibility of its binding sites. In order to improve the chemical stability in acidic solution, chemical modification via crosslinking of chitosan with ethylene glycol diglycidyl ether (EDGE) was also carried out. Most of the studies on chitosan derivatives, especially chitosan–clay beads, were conducted in single or binary metal system. In the aquatic environment, a number of metal ions are present and may compete for available adsorption sites. In addition, the presence of more than one metal in wastewater is expected to cause interactive effects depending on many factors [24].

The main objective of the study is to investigate the removal of Cu(II), Ni(II), Pb(II), and Zn(II) using non-crosslinked and crosslinked chitosan-coated montmorillonite in single and multi-metal system. The effect of ionic strength and pH on the adsorption capacity was examined. The equilibrium data of single and multi-metal system were analyzed using Langmuir and Freundlich isotherm. The experimental data for the kinetic study were evaluated using the pseudo-first-order, pseudo-second-order, and intraparticle diffusion equations. The performance of ChiMC in removing Cu(II), Ni(II), Pb(II), and Zn(II) from groundwater was evaluated as well. This information would help to determine if chitosan-coated montmorillonite could be a possible material that can be used in a permeable reactive barrier (PRB) system for the treatment of acidic plumes and contaminated groundwater.

2. Materials and methods

2.1. Chemicals and reagents

Chitosan, low molecular weight with 75–85% degree of deacetylation, was procured from Sigma-Aldrich (USA). Montmorillonite, $Cu(NO_3)_2{\cdot}2.5H_2O$, $Pb(NO_3)_2$, $Ni(NO_3)_2{\cdot}6H_2O$, and $Zn(NO_3)_2{\cdot}6H_2O$ were obtained from Ridel-de Haën, while NaOH pellets (99% purity), HCl (37% fuming), and ICP multi-element standard solution IV were purchased from Merck (Germany).

2.2. Instrumentation and equipment

A Channel Precision Oven model DV452 220 V was utilized for drying the ChiMC adsorbent. A reciprocal shaker bath YIH BT350 was used for the batch experiments. Quantitative analysis of Cu(II), Ni (II), Pb(II), and Zn(II) was done using inductively coupled plasma optical emission spectrometry (ICP-OES) Perkin Elmer Optima DV2000 Series.

2.3. Characterization of ChiMC and CChiMC

2.3.1. BET surface area analysis

Surface area analysis of ChiMC was performed using Brunauer, Emmett, and Teller (BET) multipoint technique at 77 K using N_2 adsorption using a GEMINI 2360 Micrometrics. Prior to analysis, the sample was degassed for 24 h at 343 K under vacuum.

2.3.2. Surface morphology

The scanning electron microscopy and energy dispersive X-ray spectroscopy were done using SEM–EDX Hitashi S-4800 at 20.0 kV using a tungsten filament. Prior to analysis, samples were coated with gold using a gold electric sputter coater.

2.3.3. Fourier transform infrared (FT-IR) analysis

Infrared spectra of fresh and spent ChiMC in the range of 4,000–400 cm^{-1} were acquired using Jusco FTIR-410 under 4 cm^{-1} resolution and 20 cumulative scans. Samples were mixed with KBr in a 1:10 ratio and pressed into KBr disk under vacuum.

2.4. Preparation of chitosan-coated on montmorillonite

The ChiMC beads were prepared similar to the previous method used by Wan et al. [15]. About 5.0 g of chitosan was dissolved in 5% (v/v) HCl under continuous stirring for 2 h. Montmorillonite of 100 g was added to the solution and was stirred for 3 h. NaOH solution was added slowly to the solution in a dropwise method under continuous stirring until neutral pH to precipitate chitosan onto montmorillonite. The chitosan-coated montmorillonite (ChiMC) beads were filtered and washed several times with DI water. The ChiMC beads were dried in the oven for 24 h at 65˚C and sieved.

2.5. Preparation of crosslinked chitosan-coated montmorillonite (CChiMC) beads

The method utilized in preparing crosslinked ChiMC beads was similar to the procedure described by Wan et al. [15] and Dalida et al. [19]. To obtain a 1:1 M ratio of EDGE to chitosan, 9.193 mL of EDGE solution was added to the chitosan-montmorillonite solution and stirred for 3 h. Neutralization was achieved by the dropwise addition of NaOH. The CChiMC beads were washed with DI water, filtered, and dried in the oven for 24 h and sieved.

2.6. Batch adsorption studies

2.6.1. Effect of pH

In a 125-mL Erlenmeyer flask that contains 0.100 g of ChiMC and 30 mL of metal solution with initial concentrations of 10 and 200 mg/L was agitated for 2 h under 25˚C at varying pH (2–6). The samples were filtered and the metal concentration was measured using ICP-OES with corresponding wavelengths of 213.597, 283.306, 334.558, and 231.604 nm for Cu(II), Pb(II), Zn(II), and Ni(II), respectively.

The adsorption capacity of a metal ion, q_e (mg/g) was computed using Eq. (1):

$$q_e = \frac{v(C_0 - C_e)}{m} \quad (1)$$

where C_0 is the initial concentration of the metal ion (mg/L), C_e is the final or equilibrium concentration of metal ion (mg/L), v is the volume of metal solution (mL), and m is the mass of adsorbent (g).

2.6.2. Effect of ionic strength

The effect of ionic strength (0.01–1.0 mol/L $NaNO_3$) on the adsorption capacity of ChiMC in the removal of Cu(II), Ni(II), Pb(II), and Zn(II) was investigated. About 0.100 g of ChiMC was placed in a 125 mL Erlenmeyer flask at an initial concentration of 50 mg/L and initial pH of 4.0. The flasks were agitated at 50 rpm using a shaker bath for 5 h at 25˚C.

2.6.3. Adsorption kinetic study

In single metal system, the kinetic study was performed by placing 0.100 g of adsorbent in 30 mL solution of initial concentration (10–200 mg/L) at an optimum pH 4 under varying time interval (30–300 min).

Subsequent experiments for multi-metal system were carried out under the same working conditions as that of the single metal system. Heavy metal solutions were prepared by adding 10 mg/L of each metal Cu(II), Ni(II), Pb (II), and Zn(II) to a total volume of 30 mL. About 0.100 g of adsorbent was added into the multi-metal solution and agitated at predetermined time intervals (30–300 min) at pH 4.0. The same operating conditions were applied to the kinetic study of multi-metal solution under initial concentration of 50–200 mg/L.

2.6.4. Adsorption isotherm study

Equilibrium studies for single-metal system were carried out by combining 0.10 g adsorbent and a fixed

Table 1
Background values and chemical properties of groundwater

Parameter	Values
pH	8.45
Conductivity (μS/cm)	2,978
Eh (mV)	71
Dissolved oxygen (mg/L)	1.29
Alkalinity (mg/L as CaCO3)	680
Total organic carbon, TOC (mg/L)	19.95
Ion species	
Chloride (mg/L)	298
Sulfate (mg/L)	29.5
Nitrate (mg/L)	0.45
Phosphate (mg/L)	2.19
Potassium (mg/L)	32.54
Calcium (mg/L)	26.90
Sodium (mg/L)	639.2
Heavy metals	
Iron (mg/L)	0.87
Manganese (mg/L)	0.23

volume of 30 mL metal solution that contains varying initial concentrations (5–200 mg/L) at constant temperature of 25˚C. The flasks were shaken for 5 h using 50 rpm at pH 4.

In multi-metal system, a total volume of 30 mL metal solution was prepared by adding 5 mg/L of each metal Cu(II), Ni(II), Pb(II), and Zn(II) into an Erlenmeyer flask. Then, 0.100 g adsorbent was added and agitated for 5 h at pH 4.0. Same conditions were applied to isotherm studies under different initial concentration of 50–200 mg/L.

2.7. Adsorption study of Cu(II), Ni(II), Pb(II), and Zn(II) from groundwater

Batch experiments were performed to test the capacity of ChiMC in removing Cu(II), Ni(II), Pb(II), and Zn(II) from groundwater. Groundwater was obtained from a monitoring well located in Chia Nan University Pharmacy and Science (Taiwan). The chemical composition of groundwater is given in Table 1. Groundwater was spiked with 3 mg/L Cu(II), Ni(II), Pb(II) and Zn(II).

3. Results and discussion

3.1. Surface properties of ChiMC and CChiMC

The BET surface area, average pore diameter, and zeta potential of montmorillonite, chitosan, ChiMC, and CChiMC beads have been analyzed. The surface area of montmorillonite and chitosan was 94.28 and 3.40 m^2/g, respectively. Upon coating of chitosan onto montmorillonite, the surface area of ChiMC was observed to decrease to 74.12 m^2/g. The addition of EDGE further decreased the surface area of the CChiMC beads to 20.07 m^2/g. Based on the IUPAC recommendation, total porosity of a material can be classified into three categories based on the pore diameter, d: macropores ($d > 50$ nm), mesopores (2 nm $< d <$ 50 nm), and micropores ($d < 2$ nm) [16]. The average pore diameter values of montmorillonite, chitosan, ChiMC, and CChiMC are 5.84, 6.41, 5.02, and 7.33 nm, respectively. Based on the pore diameter values, the materials are mesoporous.

The zeta potential values show that montmorillonite has the most negative surface charge of (−) 15.90, which is characteristic of this clay mineral. On the other hand, chitosan provided the lowest value of (+)0.228. The zeta potential of ChiMC beads of (−) 0.390 was almost similar to the value of chitosan, which indicates successful coating of chitosan onto montmorillonite. In the case of CChiMC, the net negative surface charge increased significantly. Upon crosslinking, the EDGE molecules interact with ChiMC mostly through the $–NH^{3+}$ groups of chitosan, which in turn increases the overall negative surface charge from (−)0.390 to (−)9.14.

3.2. SEM and elemental analysis

The results of the EDS analysis of ChiMC and CChiMC beads show that ChiMC beads have the following major elements: Si (25.12%), Al (10.26%), Fe (5.36%), Mg (1.58%), C (2.66%), and O (51.50%). Several elements such as Si, Al, Fe, Mg, and O are attributed to montmorillonite while the major elements of chitosan are C and O. Upon the addition of EGDE [molecular formula $(C_2H_4O)_nC_6H_{10}O_3$], an increase in the C (7.09%) and O (53.18%) components of the crosslinked beads was observed. However, Si and Al content decreased to 23.62 and 7.60%, which could be due to the blocking effect caused by the attachment of EGDE to the hydroxyl groups of montmorillonite, which are found mostly at the edges of silanol and aluminol groups.

Fig. 1(a) and (b) shows the surface morphology of ChiMC and CChiMC beads. The aggregated structure of ChiMC and CChiMC could be due to the hydroxylated edge–edge interaction between the silicate layers of clay and the chitosan polymer [25]. Crosslinking with EGDE molecules probably enhanced flocculation of the ChiMC beads, where the surface displays a denser texture covered by uneven ridges and cavities.

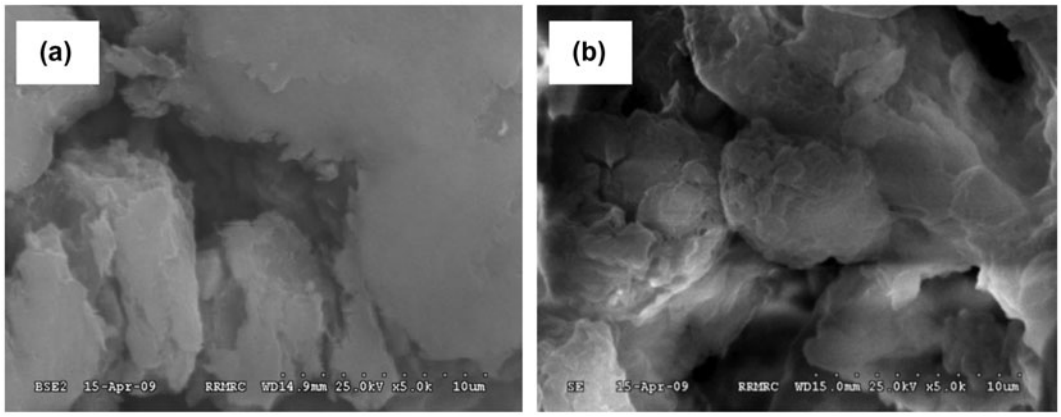

Fig. 1. SEM micrograph of (a) ChiMC and (b) CChiMC beads.

3.3. Effect of pH

The effect of varying pH (2.0–4.0) on the % removal and adsorption capacity was illustrated in Fig. 2. For ChiMC and CChiMC, uptake and % removal of the four heavy metals were observed to decrease as the pH was decreased from pH 4.0 to 2.0. The lowest adsorption capacity of Cu(II), Ni(II), Pb(II), and Zn(II) was observed at pH 2.0 for both adsorbents. An acidic solution causes the amine groups of chitosan to become protonated into amino groups ($–NH_3^+$) that are positively charged. In turn, the amino groups would exert a repulsive force on the approaching positively charged heavy metal ions that would inhibit adsorption onto the adsorbent surface. In addition, there are more H^+ ions present in acidic medium, which would provide a tighter competition for the heavy metals in binding onto the functional groups of the two adsorbents. Based on the results, the maximum adsorption capacity and % removal for ChiMC and CChiMC are attained at pH 4.0.

3.4. Effect of ionic strength

Fig. 3 shows the effect of $NaNO_3$ (0.01–1.0 mol/L) on % removal and adsorption capacity of Cu(II), Ni (II), Pb(II), and Zn(II) using ChiMC. The % removal and adsorption capacity were observed to be the highest in the absence of $NaNO_3$, and decreases gradually as the $NaNO_3$ concentration was increased from 0.01 to 1.0 mol/L. At 1.0 mol/L $NaNO_3$, a high number of Na^+ is distributed on the outer layer surrounding ChiMC beads, which further repels the approaching bivalent metal ions and causes a decrease in adsorption capacity of ChiMC.

The effect of ionic strength on the uptake capacity of ChiMC would distinguish between formation of inner and outer sphere complexes. A cation can be adsorbed as an inner sphere or an outer sphere complex. Outer sphere complexes involve weak electrostatic interaction and are strongly affected by ionic strength of the solution. On the other hand, inner sphere complexes form strong chemical bonds such as covalent or ionic binding and are weakly affected by the ionic strength [26]. Increasing the concentration of $NaNO_3$ by a hundredfold from 0.01 to 1.0 mol/L caused a slight decrease of less than 10% in the removal of the four metals. This implies that adsorption of Cu(II), Ni(II), Pb(II), and Zn(II) occurs mainly through inner sphere complexes.

3.5. Adsorption kinetics

In order to determine the rate-limiting step, kinetic models such as pseudo-first-order, pseudo-second-order, and intraparticle diffusion equations were employed to evaluate the experimental data.

The pseudo-first-order (Lagergren) equation could be expressed as Eq. (2):

$$\log\ (q_e - q_t) = \log\ q_e - \frac{k_1}{2.303} t \tag{2}$$

where k_1 (min^{-1}) is the rate constant, q_e and q_t are the adsorption capacity (mg/g) at equilibrium and at time, t (min), respectively [27].

The linear form of the pseudo-second-order equation is given by:

$$\frac{t}{q_t} = \frac{1}{k_2 q_e^2} + \frac{1}{q_e} t \tag{3}$$

where k_2 (g/mg min) is the pseudo-second-order rate constant [4].

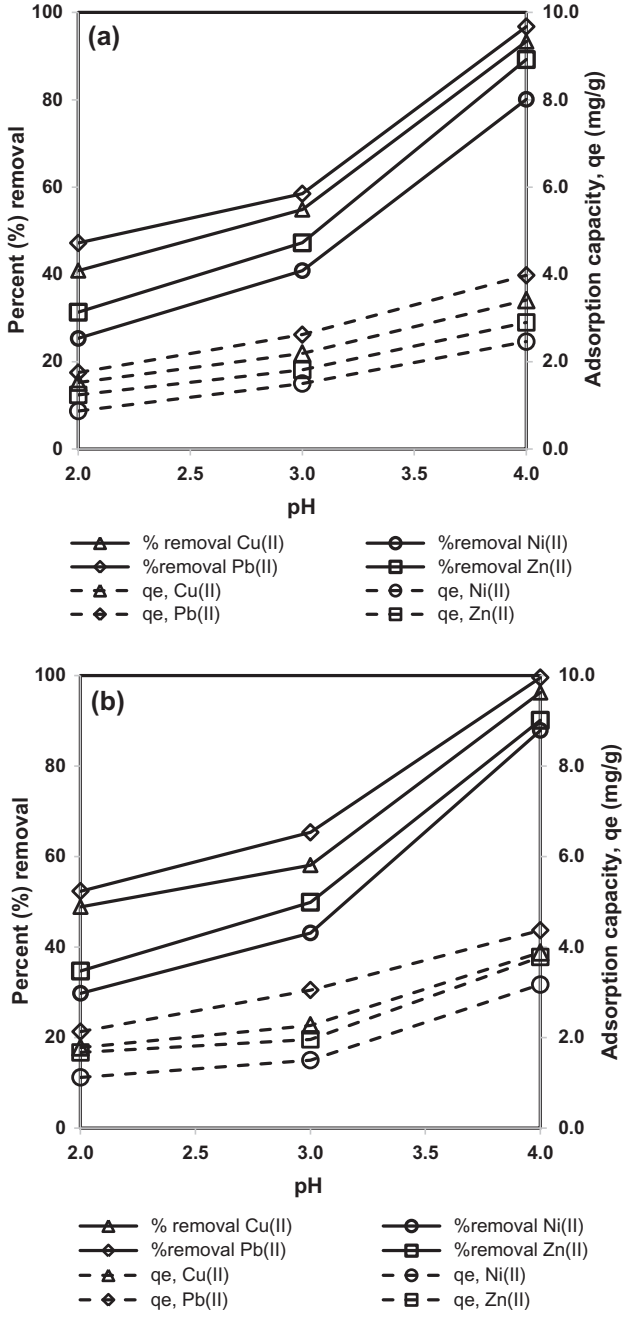

Fig. 2. Effect of pH on the adsorption capacity and percent (%) removal of Cu(II), Ni(II), Pb(II) and Zn(II) using (a) ChiMC and (b) CChiMC.

The intraparticle diffusion equation is provided by Eq. (4):

$$q_t = k_{ip} t^{0.5} + C_i \tag{4}$$

where k_{ip} (mg/g min$^{0.5}$) is the intraparticle diffusion rate constant and C_i is the thickness of boundary layer [28].

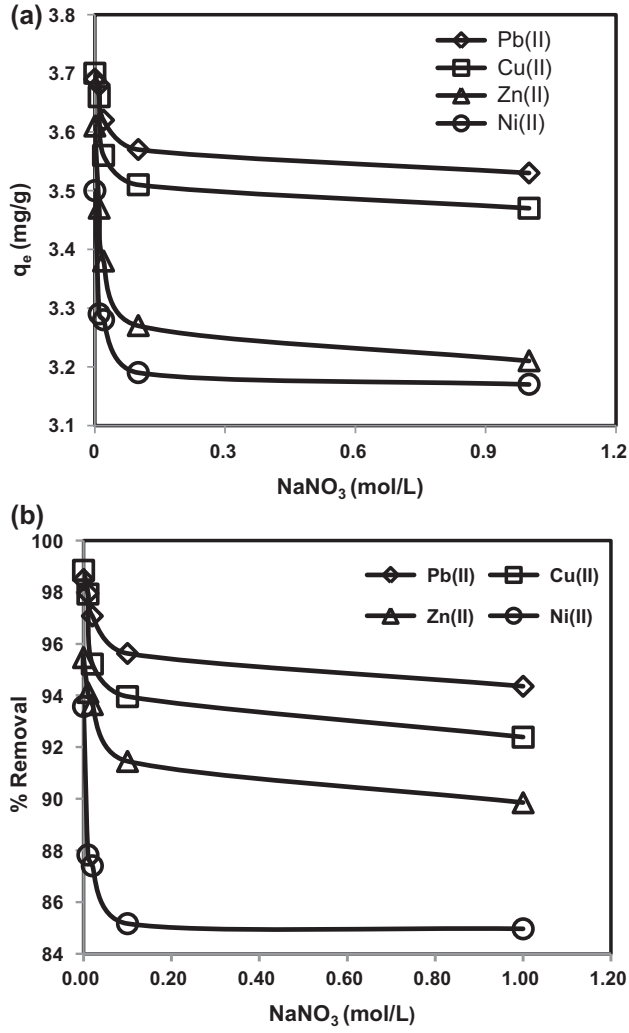

Fig. 3. Effect of $NaNO_3$ on the (a) adsorption capacity and (b) % removal of Cu(II), Ni(II), Pb(II) and Zn(II).

3.5.1. Single-metal system

The calculated kinetic parameters for the adsorption of Cu(II), Ni(II), Pb(II), and Zn(II) onto ChiMC beads are listed in Table 2 for single-metal system. It is observed that the pseudo-second-order has high correlation coefficient values ($R^2 > 0.933$). In addition, the computed theoretical q_e derived using the pseudo-second-order and experimental q_e have very similar values. Fig. 4 illustrates that the experimental data of Cu(II), Ni(II), Pb(II), and Zn(II) has a good fit with the nonlinear plots generated by the pseudo-second-order model. Therefore, it can be inferred that the rate-determining step in the adsorption of Cu(II), Ni(II), Pb(II), and Zn(II) onto ChiMC in single-metal system is chemisorption. It implies that the adsorption process involves the formation of valency forces through the

Table 2
Kinetic parameters of pseudo-first-order, intraparticle diffusion, and pseudo-second-order equation, in single-metal system using ChiMC beads

			Pseudo-first-order			Intraparticle diffusion			Pseudo-second-order		
Metal	C_0 (mg/L)	q_e, expt	k_1	q_e, theo	R^2	k_{ip}	q_e, theo	R^2	k_2	q_e, theo	R^2
Cu(II)	10	2.95	0.0021	0.57	0.501	0.0019	2.28	0.840	0.0752	2.84	0.977
	50	11.83	0.0092	3.34	0.404	0.0030	11.39	0.815	0.0283	11.90	0.998
	100	18.10	0.0115	6.22	0.562	0.0027	24.92	0.716	0.0153	18.18	0.998
	200	21.97	0.0207	13.12	0.702	0.4234	37.39	0.764	0.0105	20.83	0.972
Ni(II)	10	2.78	0.0008	0.76	0.609	0.0074	2.34	0.617	0.0736	2.77	0.980
	50	8.74	0.0115	6.47	0.920	0.0034	11.10	0.591	0.0060	9.09	0.960
	100	12.04	0.0115	8.64	0.921	0.1090	22.63	0.734	0.0052	12.50	0.972
	200	15.34	0.0092	10.81	0.862	0.7628	29.88	0.816	0.0034	15.15	0.995
Pb(II)	10	2.95	0.0023	0.75	0.428	0.0027	2.89	0.718	0.1811	2.97	0.998
	50	14.81	0.0161	2.36	0.591	0.0156	10.62	0.727	0.1548	14.92	0.999
	100	26.95	0.0253	18.66	0.930	0.0283	25.04	0.803	0.0069	27.77	0.989
	200	47.02	0.0276	33.96	0.797	0.2634	41.29	0.825	0.0032	47.61	0.953
Zn(II)	10	2.91	0.0115	1.95	0.750	0.0005	2.67	0.700	0.1204	2.91	0.973
	50	9.45	0.0092	6.82	0.878	0.0027	14.32	0.738	0.0058	9.71	0.955
	100	12.86	0.0184	11.40	0.782	0.1089	22.61	0.583	0.0055	13.33	0.933
	200	15.43	0.0138	5.90	0.498	0.5471	33.88	0.618	0.0161	15.62	0.997

exchange or sharing of electrons between the metal ions and the binding sites of the adsorbent [11].

The value of k_2 is observed to decrease with an increase in initial concentration from 10 to 200 mg/L. Occurrence of steric crowding at high initial concentration contributes to the delay in attaining equilibrium, caused by repulsive forces due to the shorter distances between the metal ions [20].

3.5.2. Multi-metal system

As shown in Table 3, the adsorption of Cu(II), Ni (II), Pb(II), and Zn(II) onto ChiMC fits well with pseudo-second-order equation, as indicated by high correlation coefficient values ($R^2 > 0.953$). Moreover, the predicted q_e values of the pseudo-second-order equation were in good agreement with the experimental q_e values. This implies that the adsorption of Cu (II), Ni(II), Pb(II), and Zn(II) in a multi-solute system follows the pseudo-second-order model. The value of k_2 was observed to decrease with increasing initial concentration for all four metals, which is the same trend in single-metal system.

3.6. Adsorption isotherm

Isotherm study describes the distribution of adsorbate molecules between liquid and the solid phase as the system reaches equilibrium [5]. The equilibrium data were analyzed using the Langmuir and Freundlich model.

Langmuir isotherm is based on the following assumptions: the model is valid only for monolayer adsorption, where all the binding sites have the same energy levels and can occupy one adsorbate molecule per site [29]. The linear equation is given as Eq. (5):

$$\frac{1}{q_e} = \frac{1}{q_{mL}} + \frac{1}{bq_{mL}C_e} \tag{5}$$

where q_{mL} is the maximum adsorption capacity at monolayer coverage (mg/g) and b (mL/mg) is the Langmuir equilibrium constant [30].

The Langmuir constant b is used to compute for a dimensionless separation factor R_L that is presented as Eq. (6):

$$R_L = \frac{1}{1 + bC_0} \tag{6}$$

The Freundlich model is an empirical equation that describes a multi-site adsorption on energetically heterogeneous surfaces [8]. The linearized form can be expressed as:

$$\log\ q_e = \log\ K_F + \frac{1}{n}\log\ C_e \tag{7}$$

where K_F and n are Freundlich constants, corresponding to relative adsorption capacity (mg/g) and adsorption intensity, respectively [31].

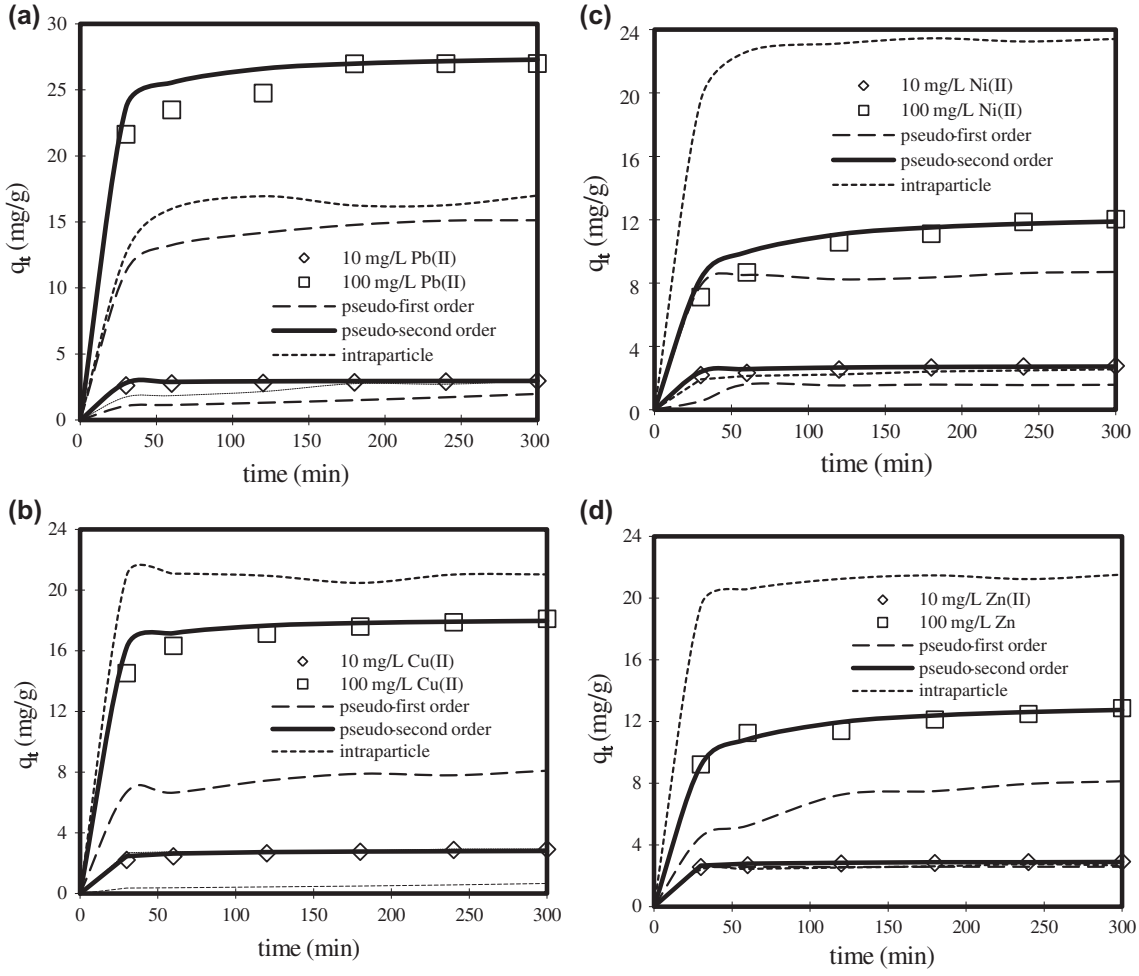

Fig. 4. Nonlinear pseudo-first-order, pseudo-second-order, and intraparticle diffusion equations for the adsorption of (a) Cu(II), (b) Ni(II), (c) Pb(II), and (d) Zn(II) ions onto ChiMC beads in single-metal system.

The Dubinin–Radushkevich (D-R) isotherm determines if the adsorption process is chemical or physical in nature through the apparent energy of adsorption [32]. It is represented in Eq. (8) [33]:

$$\ln\ q_e = \ln\ q_m - K_{DR}\varepsilon^2 \tag{8}$$

where q_m is the maximum adsorption capacity (mg/g), K_{DR} is the D-R constant (kJ^2/mol^2), and ε is the Polanyi potential. The Polanyi potential can be computed using Eq. (9):

$$\varepsilon = RT\ \ln\left[1+\frac{1}{C_e}\right] \tag{9}$$

where C_e is the equilibrium concentration of the solute (mg/L), R is the universal gas constant (kJ/mol K), and T is the absolute operating temperature (K). The mean energy of adsorption can be calculated by the following equation:

$$E = (-2K_{DR})^{-1/2} \tag{10}$$

where E is the mean energy of adsorption (kJ/mol). The value of E would determine the governing mechanism in the adsorption system, whether it is physical adsorption ($E < 8$ kJ/mol), ion-exchange mechanism (8 kJ/mol $< E <$ 16 kJ/mol) or chemisorption ($E > 16$ kJ/mol).

3.6.1. Single-metal system

The calculated Langmuir, Freundlich, and D-R parameters related to the adsorption of Cu(II), Ni(II), Pb(II), and Zn(II) in single-metal system are presented

Table 3
Kinetic parameters of pseudo-first-order and pseudo-second-order equations in multi-metal system using ChiMC beads

			Pseudo-first order			Pseudo-second order		
Metal	C_0 (mg/L)	q_e, expt	k_1	q_e, theo	R^2	k_2	q_e, theo	R^2
Cu(II)	10	3.005	0.0184	0.683	0.643	0.2480	2.747	0.982
	50	14.682	0.0161	3.715	0.304	0.1548	14.925	0.999
	100	28.355	0.0253	18.663	0.569	0.0069	27.777	0.989
	200	54.006	0.0276	33.962	0.530	0.0032	47.619	0.953
Ni(II)	10	2.974	0.0184	0.683	0.043	0.5815	2.985	0.999
	50	13.774	0.0161	3.715	0.304	0.1206	13.888	0.999
	100	26.742	0.0230	9.225	0.569	0.0761	27.027	0.999
	200	51.110	0.0253	13.458	0.530	0.1203	52.631	0.998
Pb(II)	10	2.981	0.0002	0.117	0.639	0.6200	2.985	0.999
	50	14.788	0.0138	2.666	0.519	0.1178	13.888	0.999
	100	28.867	0.0207	7.906	0.488	0.0761	27.027	0.999
	200	55.499	0.0253	11.091	0.442	0.1805	52.631	0.961
Zn(II)	10	2.976	0.0023	0.387	0.507	0.6310	2.985	0.999
	50	13.807	0.0138	2.426	0.184	0.1510	13.888	0.999
	100	26.682	0.0207	4.965	0.329	0.0945	27.027	0.999
	200	51.099	0.0230	4.518	0.223	0.2518	52.631	0.975

in Table 4. Based on the R^2 values, Langmuir isotherm provided the best fit for adsorption of Pb(II) onto ChiMC and CChiMC as well as the removal of Ni(II) using CChiMC. Meanwhile, the adsorption of Cu(II) and Zn(II) onto ChiMC and CChiMC and the removal of Ni(II) onto ChiMC correlated well with the Freundlich isotherm ($R^2 > 0.993$).

For ChiMC and CChiMC beads, the obtained q_{mL} values can be arranged in the following order: Pb(II) > Zn(II) > Cu(II) > Ni(II). The q_{mL} values of the two adsorbents do not vary considerably; though by comparison, CChiMC exhibits a slightly better adsorption capacity over ChiMC. Meanwhile, the Langmuir constant, b is related to the affinity of metal ions to the binding sites, where Pb(II) provided the highest value over Cu(II), Ni(II), and Zn(II). The high b value obtained for Pb(II) implies its high affinity to be adsorbed onto ChiMC and CChiMC, which corresponds to its high q_{mL} values. The value of the equilibrium parameter R_L would indicate if the adsorption system would be: unfavorable ($R_L > 1$), linear ($R_L = 1$), favorable ($0 < R_L < 1$), or irreversible ($R_L = 0$) [4]. The obtained R_L values are

Table 4
Isotherm parameters for adsorption of Cu(II), Ni(II), Pb(II), and Zn(II) onto ChiMC and CChiMC in single-metal system

	ChiMC				CChiMC			
Isotherm	Cu(II)	Ni(II)	Pb(II)	Zn(II)	Cu(II)	Ni(II)	Pb(II)	Zn(II)
Langmuir								
b	0.597	0.238	3.284	0.388	0.335	0.229	0.407	0.178
q_{mL}	13.04	12.18	29.85	13.49	14.16	13.93	30.30	14.71
R^2	0.987	0.986	0.995	0.987	0.982	0.985	0.983	0.988
R_L	0.008	0.021	0.002	0.013	0.015	0.045	0.023	0.076
Freundlich								
n	3.21	2.75	2.60	2.89	3.45	3.12	1.63	2.13
K_F	3.69	2.57	13.86	3.28	4.37	2.57	6.08	3.28
R^2	0.992	0.998	0.950	0.996	0.999	0.962	0.911	0.997
D-R								
q_M	8.43	6.90	15.71	6.34	8.92	7.56	17.18	7.69
E	23.18	21.68	26.52	20.27	22.85	20.93	24.01	21.54
R^2	0.935	0.870	0.893	0.931	0.907	0.897	0.850	0.871

found in the range of 0.002–0.027, which confirms that removal of Cu(II), Ni(II), Pb(II), and Zn(II) using ChiMC and CChiMC to be favorable.

For the Freundlich model, the value of n would give an indication on the favorability of adsorption. If the adsorption intensity $n < 1$, it would imply that adsorption is favorable over the whole concentration range studied. Meanwhile, a value of $n > 1$ would indicate the adsorption intensity is favorable only for high concentration range [31]. Based on the n values, adsorption of Cu(II), Ni(II), Pb(II), and Zn(II) onto ChiMC and CChiMC implies that adsorption intensity is favorable at high concentration range. The obtained K_F values, which indicate the relative sorption capacity can be arranged in the order: Pb(II) > Cu(II) > Zn (II) > Ni(II).

Among the three isotherm models applied, D-R equation provided the lowest correlation coefficient values ($R^2 < 0.82$). The values obtained for the apparent adsorption energy lie in the range between 20.27 and 26.52 kJ/mol, which indicates that chemical adsorption predominates in the Pb(II), Cu(II), Ni(II), and Zn(II) uptake of ChiMC and CChiMC.

3.6.2. Multi-metal system

Based on Table 5, Langmuir isotherm fitted well with adsorption of Cu(II), Ni(II), and Pb(II) onto ChiMC and CChiMC. On the other hand, adsorption of Zn(II) onto ChiMC and CChiMC is best described by the Freundlich model. This implies that Zn(II) could have possibly interacted with both hydroxyl (–OH) and amine ($–NH_2$) groups of ChiMC and CChiMC.

In comparison to the single-system values, the adsorption capacity of the four metals in the multi-metal system was found to be increased. These results indicated a synergistic effect where the presence of a metal ion enhances the adsorption of the other metal ions present in the solution.

3.7. FT-IR Analysis

In Fig. 5, the spectrum of unused CChiMC displays a broad band at 3,372 cm^{-1}, which corresponds to the stretching vibration of O–H and extension vibration of N–H [16]. The band shifted to 3,359 and 3,353 cm^{-1} after adsorption of Cu(II) and Pb(II), which implies that O and N atoms played a role in the uptake of metal ions. Moreover, the intensity at 3,629 cm^{-1} due to the stretching of O–H of the alcohol group, was observed to decrease to 3,617 and 3,619 cm^{-1} for the uptake of Cu(II) and Pb(II), respectively. This validates that the hydroxyl group could be involved in the heavy metal adsorption. From the spectrum of CChiMC–Pb, a new adsorption peak appeared at 1,397 cm^{-1}, which was caused by the bond flexion of C–O–H where the oxygen atom (in O–H) forms a coordination bond with Pb(II).

3.8. Selectivity for Cu(II), Ni(II), Pb(II), and Zn(II)

In the single- and multi-metal system, Pb(II) is preferentially adsorbed over Cu(II), Zn(II), and Ni(II). The affinity of ChiMC and CChiMC for the metals is arranged in the following sequence: Pb(II) > Cu(II) > Zn(II) > Ni(II). The relative selectivity of metal ions to the adsorbent could be associated with properties such as electronegativity, hydrolysis constant, and softness (Table 6). The preference for Pb(II) is due to it being readily hydrolyzed (small hydrolysis constant), high electronegativity, and softness value [32,34]. Also Pb(II) being the most electronegative among the four metals, would indicate a greater attraction and affinity to the binding sites of ChiMC and CChiMC.

Table 5
Isotherm parameters for adsorption of Cu(II), Ni(II), Pb(II), and Zn(II) onto ChiMC and CChiMC in multi-metal system

		Langmuir isotherm				Freundlich isotherm		
Adsorbent	Metal	b	q_{mL}	R^2	R_L	n	K_F	R^2
ChiMC	Cu(II)	0.00830	36.98	0.994	0.034	1.026	4.15	0.980
	Ni(II)	0.00789	33.84	0.987	0.079	1.046	3.08	0.962
	Pb(II)	0.00839	39.01	0.999	0.091	1.017	15.24	0.988
	Zn(II)	0.00817	35.48	0.981	0.011	1.043	4.12	0.999
CChiMC	Cu(II)	0.00139	38.108	0.994	0.015	3.45	4.372	0.990
	Ni(II)	0.00312	35.100	0.995	0.045	3.12	2.572	0.981
	Pb(II)	0.00415	40.291	0.989	0.023	1.63	6.081	0.953
	Zn(II)	0.00108	37.970	0.961	0.076	2.13	3.279	0.992

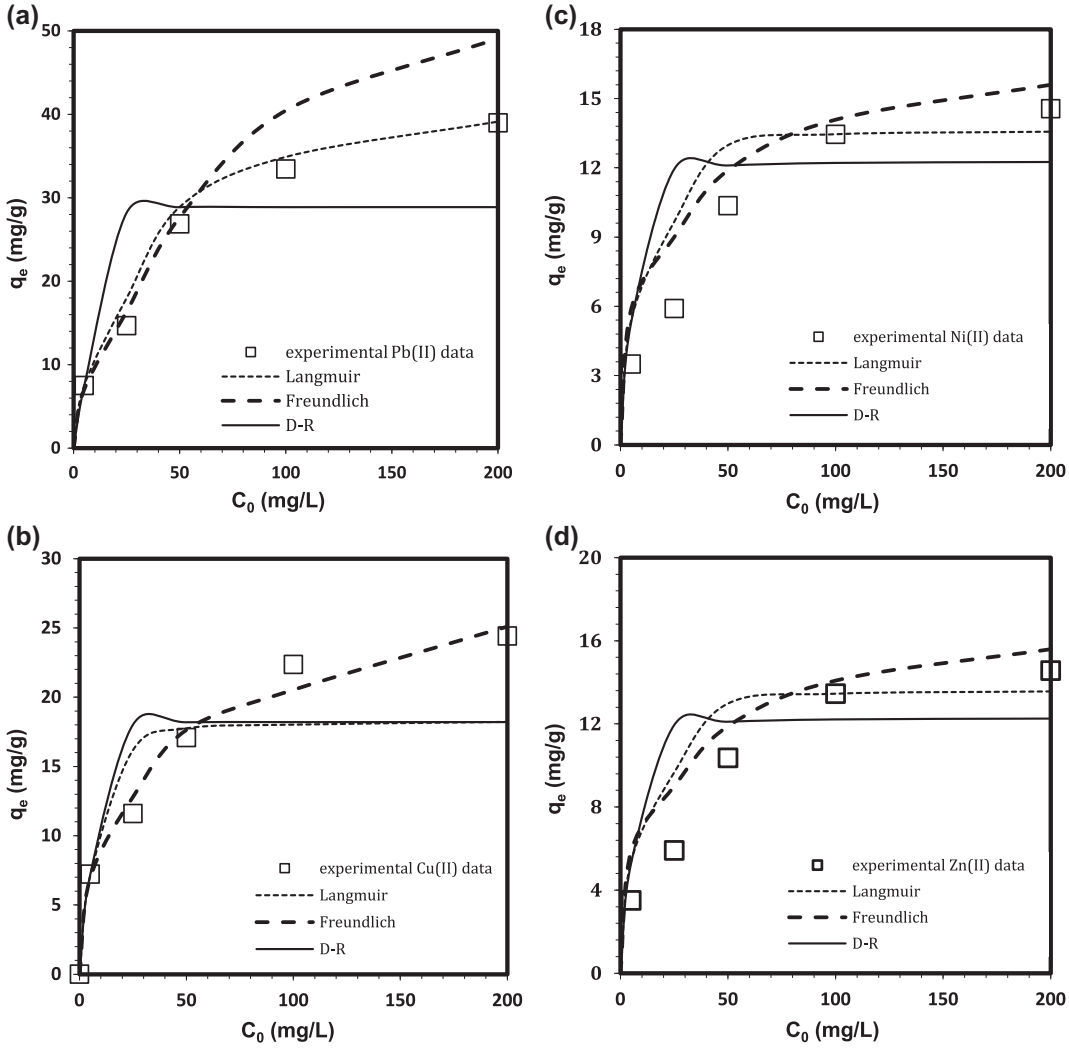

Fig. 5. Nonlinear Langmuir, Freundlich, and D-R model for the adsorption of (a) Pb(II), (b) Cu(II), (c) Ni(II), and (d) Zn (II) ions onto ChiMC beads in single-metal system.

Table 6
Metallic properties and their respective values of Pb(II), Cu(II), Ni(II), and Zn(II) [32]

Metal ion	Softness value	Hydrolysis constant	Electronegativity value
Pb(II)	3.58	7.8	2.33
Cu(II)	2.89	8.0	1.95
Ni(II)	2.82	9.9	1.91
Zn(II)	2.34	9.0	1.6

3.9. Adsorption study of Cu(II), Ni(II), Pb(II), and Zn(II) from groundwater

The adsorption efficiency of ChiMC in removing Cu(II), Ni(II), Pb(II), and Zn(II) from aqueous solution and real groundwater were compared, where the adsorbent mass was varied from 0.02 to 2.0 g (Fig. 6). The pH of the aqueous solution was set to pH 8.12, which is the same as that of groundwater. In both systems, an increase in % removal was observed with increase in adsorbent mass, due to greater number of binding sites available at 2.0 g. In the groundwater system, the maximum removal of 94.08, 92.42, 88.28,

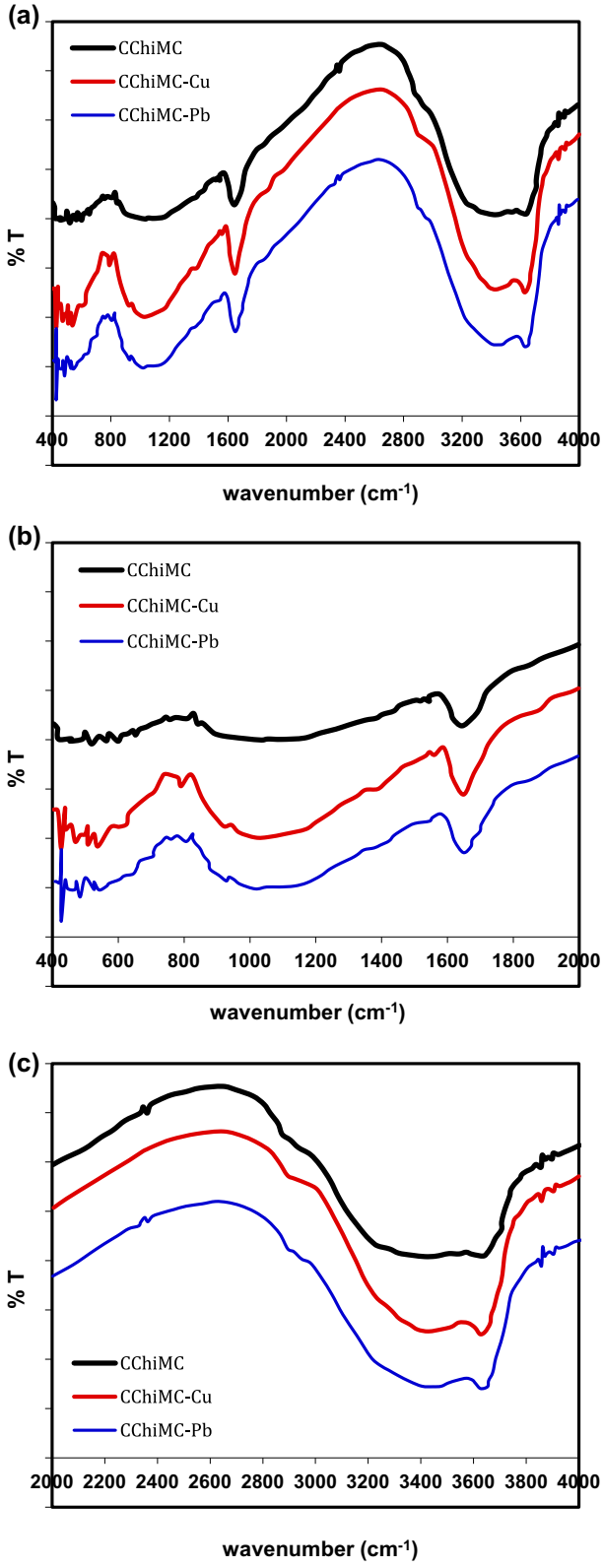

Fig. 6. FT-IR spectra of unused CChiMC, CChiMC loaded with Cu(II), and CChiMC loaded with Pb(II).

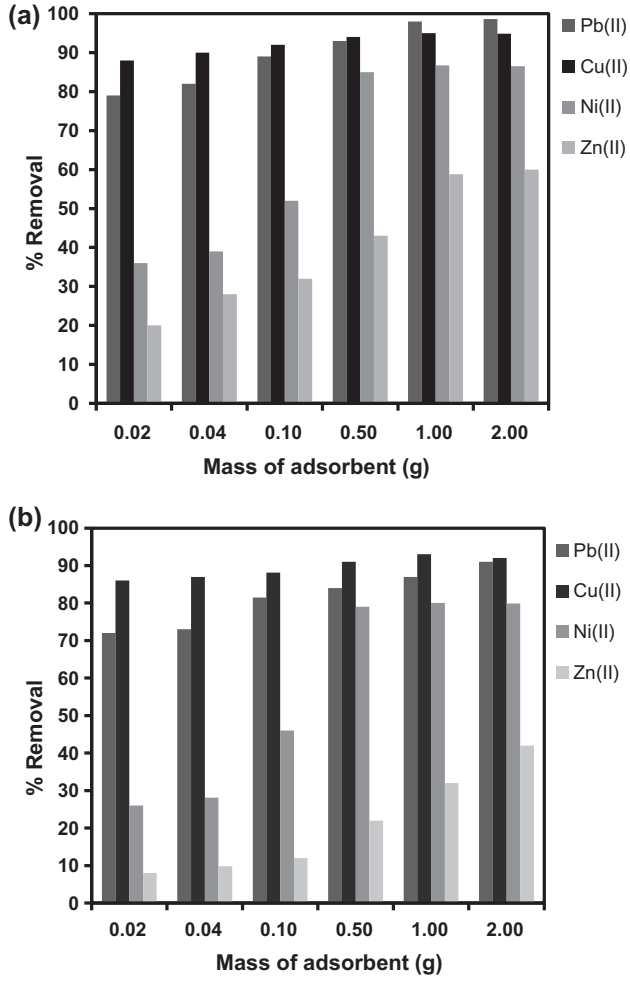

Fig. 7. Behavior of Cu(II), Ni(II), Pb(II), and Zn(II) removal in (a) groundwater and (b) aqueous solution using ChiMC ([Cu] = [Ni] = [Pb] = [Zn] = 3 mg/L; pH 8.12).

and 42.04% for Pb(II), Cu(II), Ni(II), and Zn(II) was attained at adsorbent mass of 2.0 g. However, the removal efficiency in groundwater is lower when compared with removal in aqueous solution. Existing ionic species in groundwater are Cu^{2+}, Ni^{2+}, $PbOH^{+}$, and Zn^{2+} at pH 8.12 and ORP 75 mV. Other cations such as Fe^{2+} and Mn^{2+} are also present in groundwater that could compete for adsorption sites on ChiMC, which causes lower % removal of Cu^{2+}, Ni^{2+}, $PbOH^{+}$ and Zn^{2+} (Fig. 7).

4. Conclusion

Batch experiments showed that ChiMC and CChiMC beads are effective in the removal of Cu(II), Ni(II), Pb(II), and Zn(II) from aqueous solution. An increase in ionic strength caused a decrease in %

removal of Cu(II), Ni(II), Pb(II), and Zn(II). In single-metal system, adsorption of Cu(II) and Zn(II) fitted well with the Freundlich model, while Ni(II) and Pb (II) follow the Langmuir model. An increase in adsorption capacity was observed in multi-metal system, which signifies a synergistic effect between the metal ions. Adsorption of the four metals followed the pseudo-second-order model. A maximum removal of 94.08, 92.42, 88.28, and 42.04% for Pb(II), Cu(II), Ni(II), and Zn(II) was achieved in groundwater system. Finally, the results show the possibility of using ChiMC and CChiMC as a possible material to be utilized in a PRB system.

Acknowledgement

The author would like to thank Taiwan National Science Council (NSC 99-2221-E-041-017) for their financial support.

References

[1] S. Sen Gupta, K.G. Bhattacharyya, Immobilization of Pb(II), Cd(II) and Ni(II) ions on kaolinite and montmorillonite surfaces from aqueous medium, J. Environ. Manage. 87 (2008) 46–58.
[2] G. Hilson, Pollution prevention and cleaner production in the mining industry: An analysis of current issues, J. Cleaner Prod. 8 (2000) 119–126.
[3] T.E. Norgate, S. Jahanshahi, W.J. Rankin, Assessing the environmental impact of metal production processes, J. Cleaner Prod. 15 (2007) 838–848.
[4] M.V. Dinu, E.S. Dragan, Evaluation of Cu^{2+}, Co^{2+} and Ni^{2+} ions removal from aqueous solution using a novel chitosan/clinoptilolite composite: Kinetics and isotherms, Chem. Eng. J. 160 (2010) 157–163.
[5] W.S. Wan Ngah, S. Fatinathan, Adsorption characterization of Pb(II) and Cu(II) ions onto chitosan-triphosphate beads: Kinetic, equilibrium and thermodynamic studies, J. Environ. Manage. 91 (2010) 958–969.
[6] S.R. Popuri, Y. Vijaya, V.M. Boddu, K. Abburi, Adsorptive removal of copper and nickel ions from water using chitosan coated PVC beads, Bioresour. Technol. 100 (2009) 194–199.
[7] O.S. Amuda, A.A. Giwa, I.A. Bello, Removal of heavy metal from industrial wastewater using modified activated coconut shell carbon, Biochem. Eng. J. 36 (2007) 174–181.
[8] P. Sathishkumar, M. Arulkumar, T. Palvannan, Utilization of agro-industrial waste *Jatropha curcas* pods as an activated carbon for the adsorption of reactive dye Remazol Brilliant Blue R (RBBR), J. Cleaner Prod. 22 (2012) 67–75.
[9] K.G. Bhattacharyya, S.S. Gupta, Kaolinite, montmorillonite, and their modified derivatives as adsorbents for removal of Cu(II) from aqueous solution, Sep. Purif. Technol. 50 (2006) 388–397.
[10] W.S. Wan Ngah, S. Fatinathan, Pb(II) biosorption using chitosan and chitosan derivative beads: Equilibrium, ion exchange and mechanism studies, J. Environ. Sci. 22 (2010) 338–346.
[11] C. Septhum, S. Rattanaphani, J.B. Bremner, V. Rattanaphani, An adsorption study of Al(III) ions onto chitosan, J. Hazard. Mater. 148 (2007) 185–191.
[12] T.W. Chung, C.H. Chang, C.W. Ho, Incorporating chitosan (CS) and TPP into silk fibroin (SF) in fabricating spray-dried microparticles prolongs the release of a hydrophilic drug, J. Taiwan Inst. Chem. Eng. 42 (2011) 592–597.
[13] Y.C. Kuo, C.C. Wang, Effect of bovine pituitary extract on the formation of neocartilage in chitosan/gelatin scaffolds, J. Taiwan Inst. Chem. Eng. 41 (2010) 150–156.
[14] N. Gupta, A.K. Kushwaha, M.C. Chattopadhyaya, Adsorptive removal of Pb^{2+}, Co^{2+} and Ni^{2+} by hydroxyapatite/chitosan composite from aqueous solution, J. Taiwan Inst. Chem. Eng. 43 (2012) 125–131.
[15] M.W. Wan, C.C. Kan, B.D. Rogel, M.L. Dalida, Adsorption of copper(II) and lead(II) ions from aqueous solution on chitosan-coated sand, Carbohydr. Polym. 80 (2010) 891–899.
[16] A. Kamari, W.S. Ngah, Isotherm, kinetic and thermodynamic studies of lead and copper uptake by H_2SO_4 modified chitosan, Colloids Surf., B 73 (2009) 257–266.
[17] M.O. Machado, E.C.N. Lopes, K.S. Sousa, C. Airoldi, The effectiveness of the protected amino group on crosslinked chitosans for copper removal and the thermodynamics of interaction at the solid/liquid interface, Carbohydr. Polym. 77 (2009) 760–766.
[18] A.H. Chen, S.C. Liu, C.Y. Chen, C.Y. Chen, Comparative adsorption of Cu(II), Zn(II), and Pb(II) ions in aqueous solution on the crosslinked chitosan with epichlorohydrin, J. Hazard. Mater. 154 (2008) 184–191.
[19] M.L. Dalida, A.F. Mariano, C.M. Futalan, C.C. Kan, W.C. Tsai, M.W. Wan, Adsorptive removal of Cu(II) from aqueous solutions using non-crosslinked and crosslinked chitosan-coated bentonite beads, Desalination 275 (2011) 154–159.
[20] C.M. Futalan, C.C. Kan, M.L. Dalida, K.J. Hsien, C. Pascua, M.W. Wan, Comparative and competitive adsorption of copper, lead and nickel using chitosan immobilized on bentonite, Carbohydr. Polym. 83 (2011) 528–536.
[21] N. Grisdanurak, S. Akewaranugulsiri, C.M. Futalan, W.C. Tsai, C.C. Kan, C.W. Hsu, M.W. Wan, The study of copper adsorption from aqueous solution using crosslinked chitosan immobilized on bentonite, J. Appl. Polym. Sci. 125 (2011) E132–E142.
[22] K. Swayampakula, V.M. Boddu, S.K. Nadavala, K. Abburi, Competitive adsorption of Cu(II), Co(II) and Ni(II) from their binary and tertiary aqueous solutions using chitosan-coated perlite beads as biosorbent, J. Hazard. Mater. 170 (2009) 680–689.
[23] H. Gecol, P. Miakatsindila, E. Ergican, S.R. Hiibel, Biopolymer coated clay particles for the adsorption of tungsten from water, Desalination 197 (2006) 165–178.
[24] B.Y.M. Bueno, M.L. Torem, F. Molina, L.M.S. de Mesquita, Biosorption of lead(II), chromium(III) and copper(II) by *R. opacus*: Equilibrium and kinetic studies, Miner. Eng. 21 (2008) 65–75.
[25] S.F. Wang, L. Shen, Y.J. Tong, L. Chen, I.Y. Phang, P.Q. Lim, T.X. Liu, Biopolymer chitosan/montmorillonite nanocomposites: Preparation and characterization, Polym. Degrad. Stab. 90 (2005) 123–131.

[26] D. Tiwari, H.U. Kim, S.M. Lee, Removal behavior of sericite for Cu(II) and Pb(II) from aqueous solutions: Batch and column studies, Sep. Purif. Technol. 57 (2007) 11–16.
[27] M. Benavente, L. Moreno, J. Martinez, Sorption of heavy metals from gold mining wastewater using chitosan, J. Taiwan Inst. Chem. Eng. 42 (2011) 976–988.
[28] B.H. Hameed, I.A.W. Tan, A.L. Ahmad, Adsorption isotherm, kinetic modeling and mechanism of 2,4,6-trichlorophenol on coconut-husk based activated carbon, Chem. Eng. J. 144 (2008) 235–244.
[29] J. Febrianto, A.N. Kosasih, J. Sunarso, Y.H. Ju, N. Indraswati, S. Ismadji, Equilibrium and kinetic studies in adsorption of heavy metals using biosorbent: A summary of recent studies, J. Hazard. Mater. 162 (2009) 616–645.
[30] F. Qin, B. Wen, X.Q. Shan, Y.N. Xie, T. Liu, S.Z. Zhang, S.U. Khan, Mechanisms of competitive adsorption of Pb, Cu, and Cd on peat, Environ. Pollut. 144 (2006) 669–680.
[31] W.S. Wan Ngah, S. Fatinathan, Adsorption of Cu(II) ions in aqueous solution using chitosan beads, chitosan-GLA beads and chitosan-alginate beads, Chem. Eng. J. 143 (2008) 62–72.
[32] S.M. Musyoka, H. Mittal, S.B. Mishra, J.C. Ngila, Effect of functionalization on the adsorption capacity of cellulose for the removal of methyl violet, Int. J. Biol. Macromol. 65 (2014) 389–397.
[33] C. Han, H. Li, H. Pu, H. Yu, L. Deng, S. Huang, Y. Luo, Synthesis and characterization of mesoporous alumina and their performances for removing arsenic (V), Chem. Eng. J. 217 (2013) 1–9.
[34] A.R. Usman, The relative adsorption selectivities of Pb, Cu, Zn, Cd and Ni by soils developed on shale in New Valley, Egypt, Geoderma 144 (2008) 334–343.